ompton scattering on the proton and light nuclei in the Delta-resonance region

holten, O; Kondratyuk, S; Van Daele, L; Van Neck, D; Waroquier, M; Korchin, AY

blished in:
a Physica Polonica B

blication date:
02

COMPTON SCATTERING ON THE PROTON AND LIGHT NUCLEI IN THE Δ-RESONANCE REGION*

O. Scholten

Kernfysisch Versneller Instituut, University of Groningen
9747 AA Groningen, The Netherlands

S. Kondratyuk

TRIUMF, 4004 Wesbrook Mall, Vancouver, British Columbia
Canada V6T 2A3

L. Van Daele, D. Van Neck, M. Waroquier

Department of Subatomic and Radiation Physics, University of Gent
B-9000 Gent, Belgium

and A.Yu. Korchin

National Science Center 'Kharkov Institute of Physics and Technology'
61108 Kharkov, Ukraine

(Received January 22, 2002)

Microscopic calculations of Compton scattering on the free proton and light nuclei are presented. For the description of Compton scattering on the proton the conventional K-matrix approach and the "Dressed K-Matrix" model are introduced. The latter approach can be used to calculate polarizabilities as well as Compton scattering for photon energies upto 1 GeV since it obeys the symmetry properties which are appropriate in the different energy regions. In particular, crossing symmetry, gauge invariance and unitarity are satisfied. The extent of violation of analyticity (causality) is used as an expansion parameter. Coherent Compton scattering on light nuclei at 200–300 MeV is studied in the impulse approximation and is shown to be a sensitive probe of the in-medium properties of the Δ-resonance. Modifications of the properties of the Δ-resonance due to the nuclear medium are accounted for through the self-energy operator of the Δ. The dominant medium effects such as the Pauli blocking effects in the decay width, effective nucleon mass and particle–hole excitations in the pion propagator are consistently included in nuclear matter.

PACS numbers: 11.55.Fv, 13.40.Gp, 13.60.Fz, 25.20.Dc

* Presented at the VI TAPS Workshop, Krzyże, Poland, September 9–13, 2001.

1. Outline

In this contribution a few topics are discussed which, although seemingly unrelated, are unified by the focus on interaction of photons with nuclear systems and by the use of similar calculational techniques. First we discuss the K-matrix approach to Compton and pion scattering on the free proton. In such a relatively simple relativistic coupled channels approach most of the important symmetries, such as unitarity, crossing and gauge invariance, are obeyed. In the present approach a large number of resonances are included in the description where the Δ-resonance is of particular interest for the later discussions of the in-medium properties.

In Section 4 an extension of this approach, the "Dressed K-Matrix Model", is discussed where, without violating the other symmetries, an additional constraint, that of analyticity (or causality), is incorporated approximately. In this approach dressed self-energies and form factors are included in the K-matrix. These functions are calculated self-consistently in an iteration procedure where dispersion relations are used at each recursion step to relate real and imaginary parts.

The properties of the Δ-resonance in the medium are calculated in Section 5 using a Δ–hole model. Two processes compete in determining the in-medium width as function of density: the decay width narrows in the medium due to the Pauli principle, and the spreading width strongly increases with density. We incorporated mean-field effects through a nucleon effective mass. From the width, *i.e.* the imaginary part of the self energy, the real part is calculated via a dispersion relation, which is similar to the dressing procedure in the vacuum. However, presently self-consistency is not taken into account in this calculation, in which respect it differs from the "Dressed K-Matrix" approach.

To compare our prediction with experiment we have used the impulse and factorization approximations in which the coherent cross section on a nucleus is calculated through scattering off a moving nucleon with momentum chosen such that — without modifying the energy–momentum transferred to the nucleus — the energy–momentum conservation on the nucleon is fulfilled. To describe Compton scattering on the moving nucleon we employ the aforementioned K-matrix approach where, however, a medium-modified Δ self-energy is used. This procedure ensures that background processes are included in the description and that furthermore gauge invariance is obeyed at the one-body level.

2. The K-matrix approach

In this section only a short overview of the K-matrix model is presented with emphasis on the application to Compton scattering. A more complete overview of the model and extensive comparisons with data is presented by Bennhold in his contribution to this workshop.

In K-matrix models the T-matrix is written in the form,

$$T = (1 - Ki\delta)^{-1} K \,, \tag{1}$$

where δ indicates that the intermediate particles have to be taken on the mass shell and all physics is put in the kernel, the K-matrix. It is straightforward to check that $S = 1 + 2iT$ is unitary provided that the kernel K is Hermitian. Since Eq. (1) involves integrals only over on-shell intermediate particles, it reduces to a set of algebraic equations when one is working in a partial wave basis. When both the π–N and γ–N channels are open, the coupled-channel K-matrix becomes a 2×2 matrix in the channel space, *i.e.*

$$K = \begin{bmatrix} K_{\gamma\gamma} & K_{\gamma\pi} \\ K_{\pi\gamma} & K_{\pi\pi} \end{bmatrix} . \tag{2}$$

It should be noted that due to the coupled channels nature of this approach the widths of resonances are generated dynamically.

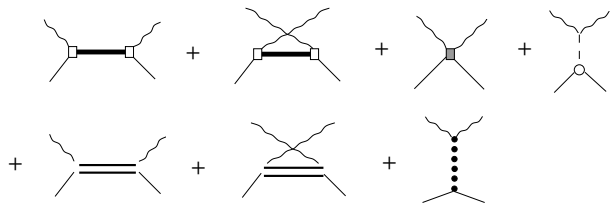

Fig. 1. The sum of diagrams included in the K-matrix for Compton scattering. A nucleon propagator is denoted by a solid line, the wiggly lines are photons, the dashed lines denote pions, the dotted lines are σ mesons, and the double lines denote baryon resonances where a full spectrum has been included.

In traditional K-matrix models the kernel, the K-matrix, is built from tree-level diagrams [1–4]. In the present investigation the type of diagrams included in $K_{\gamma\gamma}$ are similar to that of Ref. [4] except that the Δ is treated now as a genuine spin-3/2 resonance [5] in order to be compatible with the later treatment of the in-medium Δ-resonance. This K-matrix is indicated in Fig. 1. Most of the (non-strange) resonances below 1.7 GeV have been included. The different coupling constants were fitted to reproduce pion scattering, pion photoproduction and Compton scattering on the nucleon. A comparable fit to the data as in Ref. [4] could be obtained. In Fig. 2 the results for Compton scattering are compared to data.

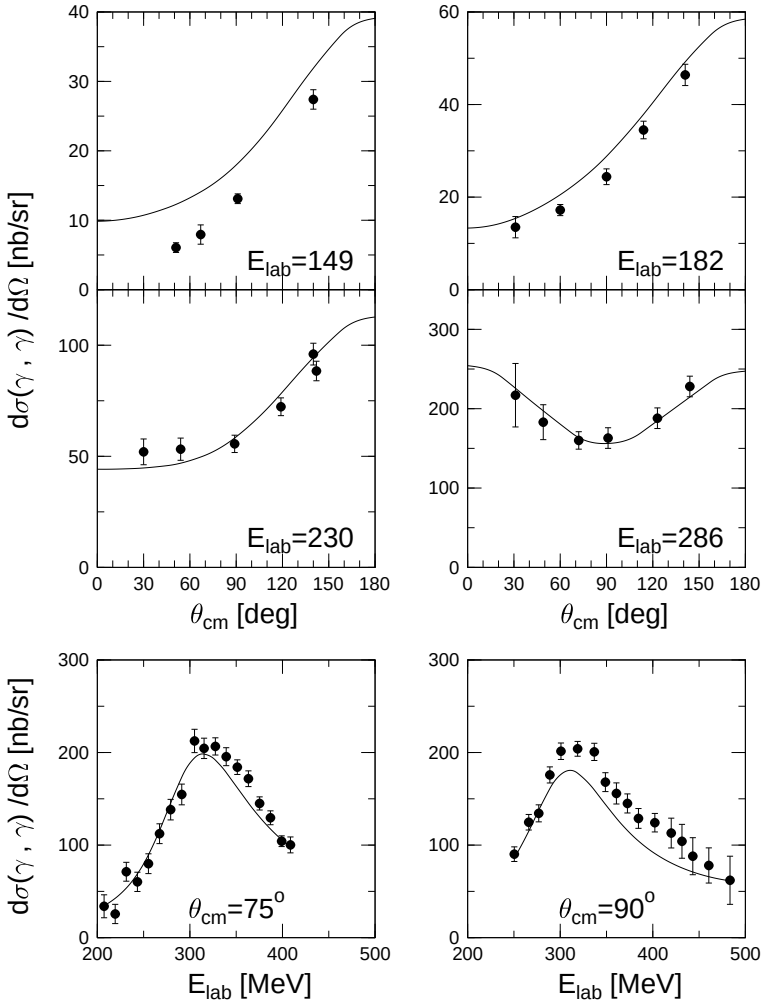

Fig. 2. The calculated cross section for Compton scattering off the proton as a function of angle at fixed photon energy, and as a function of photon energy at fixed angle. Data are taken from Ref. [11].

3. Basic symmetries

A realistic scattering amplitude for a particular process should obey certain symmetry relations, such as Unitarity, Covariance, Gauge invariance, Crossing symmetry and Causality. In the following each of these symmetries will be shortly addressed, stating its physical significance. It is also indicated which of these is obeyed by the K-matrix approach discussed in

the previous section. The comparative success of the K-matrix formalism can be regarded as due to the large number of symmetries which are being obeyed. A violation of anyone of these symmetries will directly imply some problems in applications. Improvements are thus important.

3.1. Unitarity

The unitarity condition for the scattering matrix S reads $S^\dagger S = 1$. Usually one works with the T-matrix operator which can be defined as $S = 1 + 2\,i\,T$, and the unitarity condition is rewritten as $2i(TT^\dagger)_{fi} = T_{fi} - T^*_{if}$. If the T-matrix is symmetric (which is related to time-reversal symmetry), the last formula becomes Im $T_{fi} = \sum_n T_{fn} T^*_{in}$, where the sum runs over physical intermediate states. The latter relation is the generalization of the well-known optical theorem for the scattering amplitude. Unitarity can only be obeyed in a coupled channel formulation; the imaginary part of the amplitude "knows" about the flux that is lost in other channels.

In the K-matrix formalism the T-matrix is expressed as $T = \frac{K}{1-i\,K}$ which implies that $S = \frac{1+i\,K}{1-i\,K}$ is clearly unitary provided the kernel K is Hermitian. This kernel is a matrix, where the different rows and columns correspond to different physical outgoing (incoming) channels. The coupled-channels nature is thus inherent in such an approach. As explained earlier the kernel is usually written as the sum of all possible tree-level diagrams. In a partial-wave basis K is a matrix of relatively low dimensionality and the inverse, implied in the calculation of the T-matrix, can readily be calculated.

Above the two-pion production threshold, sizable inelasticities are observed for pion scattering in certain partial waves. Since the 2-π production channel is not explicitly taken into account, purposely unitarity is broken by adding an energy-dependent imaginary part to the self energies of resonances (except for the Delta resonance) corresponding to the decay outside the model space [4].

3.2. Covariance

The scattering amplitude is said to be covariant if it transforms properly under Lorentz transformations. As a consequence the description of the reaction observables is independent of the particular reference frame chosen for the calculations. It naturally implies that relativistic kinematics is used.

Since the appropriate four-vector notation and γ-matrix algebra are used throughout our calculation, the condition of Lorentz covariance is fulfilled.

3.3. Gauge invariance

Gauge invariance means that there is certain freedom in the choice of the electromagnetic field, not affecting the observables. Its implication is current conservation, $\nabla\vec{J} = \frac{\partial\rho}{\partial t}$, or in four-vector notation, $\partial_\mu J^\mu = 0$. Using the well known correspondence between momenta and derivatives, current conservation can be re-expressed as $k_\mu J^\mu = 0$. If the electromagnetic current obeys this relation it can easily be shown that observables, such as a photoproduction cross section, are independent of the particular gauge used for constructing the photon polarization vectors.

One of the sources for violation of gauge invariance is the form factors used in the vertices. A form factor implies that at a certain (short range) scale a particle appears 'fuzzy'. At distances smaller than this scale deviations from a point-like structure are important; however in the formulation the dynamics at this short scale is not sufficiently accurate. For one thing, the flow of charge at this scale is not properly accounted for, implying violation of charge conservation. To correct for this, so-called contact terms are usually included in the K-matrix kernel. In the present model these contact terms are constructed using the minimal substitution rules. The corresponding T-matrix, as well as the observables, are independent of the photon gauge.

3.4. Crossing symmetry

Physical consequences of the crossing symmetry are more difficult to explain. It basically means that in a proper field-theoretical framework the scattering amplitudes of processes in the so-called crossed channels can be obtained from each other by appropriate replacements of kinematics. This assumes that the amplitude can be analytically continued from the physical region of one channel to the physical regions of other channels. An example of the crossed channels is $\gamma N \to \pi N$, $\pi N \to \gamma N$ and $N\bar{N} \to \gamma\pi$.

Crossing symmetry puts a direct constraint on the amplitude for the case that direct and crossed channels are identical, as for example for the processes $\pi N \to \pi N$ or $\gamma N \to \gamma N$. In these reactions crossing symmetry leads to important symmetry properties of the amplitudes under interchange of s and u variables. Due to the fact that in the K-matrix formalism the rescattering diagrams which are taken into account have only on-shell intermediate particles, it can be shown that the s–u crossing symmetry is obeyed provided that the kernel itself is crossing symmetric. Since the latter is the case, crossing symmetry is obeyed.

3.5. Analyticity

Analyticity of the scattering matrix is not really a symmetry. Rather, it requires that the amplitude be an analytic function of the energy variable and in particular that it obeys dispersion relations. The physics of analyticity is closely related to causality of the amplitude as is illustrated in the following example.

Assume that a signal is emitted by an antenna at time $t = 0$. At all subsequent times the signal is given by a function $F(t)$ while causality requires that at earlier times there was no signal, $F(t < 0) = 0$. This signal can be Fourier-transformed, $f(\omega) = \int_0^{+\infty} dt\, \mathrm{e}^{i\omega t} F(t)$ to explicitly show its energy or frequency dependence. Note that the integration region from $t = -\infty$ to $t = 0$ gives zero contribution due to the causality requirement. This transformation can also be considered for complex values of ω. Since the integration interval runs only over positive values for t the Fourier integral exists and is a well behaving function for all complex values of energy ω for which Im $(\omega) > 0$ *i.e.* it is an analytic function in the upper half plane. For such a function contour integrals in the complex ω plane can be performed and the function obeys the Cauchy theorem which in this context is usually formulated as a dispersion relation,

$$\mathrm{Re}\, f(\omega) = \frac{\mathcal{P}}{\pi} \int_{-\infty}^{+\infty} d\omega' \frac{\mathrm{Im} f(\omega')}{\omega' - \omega}$$

showing that for an analytic function the real and imaginary parts are closely related. For example, if the imaginary part of an analytic function is given by the curve on the left-hand side of Fig. 3 the real part of this function is given by the right-hand side.

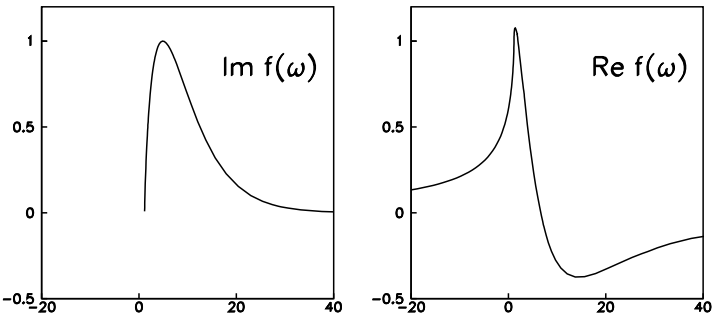

Fig. 3. An example of the real and imaginary parts of an analytic function which are related through a dispersion relation.

In the traditionally used K-matrix approaches the analyticity constraint is badly violated. The origin of this is explained in the following.

In a field-theoretical calculation of a scattering amplitude one includes rescattering contributions of intermediate particles which are expressed as loop integrals. In Fig. 4 a typical loop contribution to the self energy is shown. Ignoring terms in the numerator which are irrelevant for the analyticity properties, the corresponding integral can be expressed as

$$J(p^2) = \int d^4k \, \frac{1}{[k^2 - \mu^2 + i\varepsilon]\,[(p-k)^2 - m^2 + i\varepsilon]} = \mathrm{Re}\, J(p^2) + i\mathrm{Im}\, J(p^2), \tag{3}$$

where the right-hand side in this equation and in Fig. 4 expresses the fact that this integral has a real and an imaginary part, each of which corresponds to some particular physics. The imaginary part of the integral arises from the integration region where the denominators vanish, corresponding to four-momenta k where the intermediate particles in the loop are on the mass shell, or equivalently, are physical particles with $k^2 = \mu^2$ and $(p-k)^2 = m^2$. Conventionally this is indicated by placing a slash through the loop (see Fig. 4) to indicate that the loop can be cut at this place since it corresponds to a physical state. The other parts of the integration region contribute to the real part of the integral. In the latter case the particles in the loop are off the mass shell.

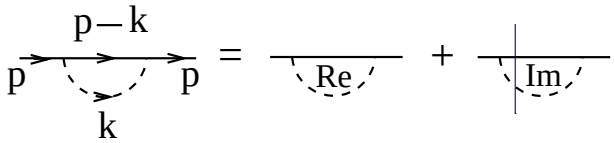

Fig. 4. Loop integral contributing to the self energy.

It can be shown that the K-matrix formulation for the T-matrix corresponds to including only the imaginary (or cut-loop) contributions of a certain class of loop diagrams. This guarantees (as was shown before) that unitarity is obeyed. Analyticity of the scattering amplitude is however violated due to ignoring the real contributions of these loop integrals. As a consequence causality will be violated!

To (partially) recover analyticity of the scattering amplitude the so-called "Dressed K-matrix approach" [9] has been developed. It is described in the following section.

4. The dressed K-matrix model

As discussed in the previous section, the coupled channels K-matrix approach is quite successful in reproducing Compton scattering. However it fails in predicting nucleon polarizabilities. The reason is that, in spite of

the many symmetry properties that are satisfied, analyticity or causality of the amplitude is badly violated. In the "Dressed K-matrix" approach the constraint of analyticity is incorporated in an approximate manner without spoiling the other symmetries. In fact analyticity is used as a kind of expansion parameter where presently only the leading contributions are included. The ingredients of the Dressed K-Matrix Model were described in Refs. [6–8] and the main results were presented in Ref. [9]. The essence of this approach lies in the use of *dressed* vertices and propagators in the kernel K.

The objective of dressing the vertices and propagators is solely to improve on the analytic properties of the amplitude. The imaginary parts of the amplitude are generated through the K-matrix formalism (as imposed by unitarity) and correspond to cut loop corrections where the intermediate particles are taken on their mass shell. The real parts have to follow from applying dispersion relations to the imaginary parts. We incorporate these real parts as real vertex and self-energy functions. Investigating this in detail (for a more extensive discussion we refer to [6]) shows that the dressing can be formulated in terms of coupled equations, schematically shown in Fig. 5, which generate multiple overlapping loop corrections. The coupled nature of the equations is necessary to obey simultaneously unitarity and analyticity at the level of vertices and propagators.

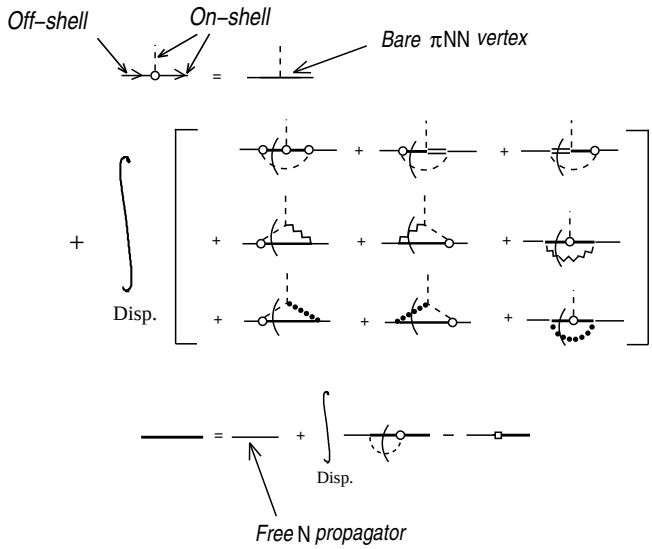

Fig. 5. Graphical representation of the equation for the dressed irreducible πNN vertex, denoted by an open circle, and the dressed nucleon propagator, denoted by a solid line. The dashed lines denote pions, the double lines denote Δs and the zigzag and dotted lines are ρ and σ mesons, respectively. The resonance propagators are dressed. The last term in the second equation denotes the counter-term contribution to the nucleon propagator, necessary for the renormalization.

The equations presented in Fig. 5 are solved by iteration where every iteration step proceeds as follows. The imaginary — or pole — contributions of the loop integrals for both the propagators and the vertices are obtained by applying cutting rules. Since the outgoing nucleon and the pion are on-shell, the only kinematically allowed cuts are those shown in Fig. 5. The principal-value part of the vertex (*i.e.* the real parts of the form factors) and self-energy functions are calculated at every iteration step by applying dispersion relations to the imaginary parts just calculated, where only the physical one-pion–one-nucleon cut on the real axis in the complex p^2-plane is considered. These real functions are used to calculate the pole contribution for the next iteration step. This procedure is repeated to obtain a converged solution *i.e.* the square deviation between the different vertex and self-energy functions for two successive iterations is less than a certain limit. We consider irreducible vertices, which means that the external propagators are not included in the dressing of the vertices.

Bare πNN form factors have been introduced in the dressing procedure to regularize the dispersion integrals. The bare form factor reflects physics at energy scales beyond those of the included mesons and which has been left out of the dressing procedure. One thus expects a large width for this factor, as is indeed the case.

The dressed nucleon propagator is renormalized (through a wave function renormalization factor Z and a bare mass m_0) to have a pole with a unit residue at the physical mass. The nucleon self-energy is expressed in terms of self-energy functions $A(p^2)$ and $B(p^2)$ as $\Sigma_N(p) = A_N(p^2)\not{p} + B_N(p^2)\ m$.

The procedure of obtaining the γNN vertex [7] is in principle the same as for the πNN vertex. Contact $\gamma\pi NN$ and $\gamma\gamma NN$ vertices, necessary for gauge invariance of the model, are constructed by minimal substitution in the dressed πNN vertex and nucleon propagator, as was explained in [7].

The present procedure restores analyticity at the level of one-particle reducible diagrams in the T-matrix. In general, violation due to two- and more-particle reducible diagrams can be regarded as higher order corrections. An important exception to this general rule is formed by, for example, diagrams where both photons couple to the same intermediate pion in a loop (so-called "handbag" diagrams). This term is exceptional since at the pion threshold the S-wave contribution is large, due to the non-zero value of the $E_{0+}^{1/2}$ multipole (notation: Electric radiation, where the pion–nucleon state has $l = 0$ and thus parity $\pi = (-1)^{(l+1)} = -$, $J = l + 1/2 = 1/2$ and $T = 1/2$) in pion-photoproduction, leading to a sharp near-threshold energy dependence of the related f_{EE}^{1-} Compton amplitude [13] (notation: Electric in and out-going photon with orbital angular momentum $l = 1$ and thus parity $\pi = (-1)^l = -$, and total angular momentum $J = l - 1/2 = 1/2$). In the K-matrix formalism, the imaginary (pole) contribution of this type of

diagrams is taken into account. Not including the real part of such a large contribution would entail a significant violation of analyticity. To correct for this, the $\gamma\gamma NN$ vertex also contains the (purely transverse) "cusp" contact term whose construction is described in Section 4 of Ref. [7]. Since, due to chiral symmetry, the S-wave pion scattering amplitude vanishes at threshold, the mechanism that gives rise to the important "cusp" term in Compton scattering does not contribute to $\pi\pi NN$ or $\pi\gamma NN$ contact terms. The analogons to the "cusp" $\gamma\gamma NN$ term will thus be negligible and have therefore not been considered.

4.1. Results

Results for pion–nucleon scattering and pion-photoproduction obtained in the dressed K-matrix model and in the traditional K-matrix approach are of comparable quality. One should, however, expect the two approaches to have significant differences for Compton scattering since for this case constraints imposed by analyticity will be most important [12, 13].

The effect of the dressing on the f_{EE}^{1-} amplitude can be seen in Fig. 6, where also the results of dispersion analyses are quoted for comparison. Note that the imaginary parts of f_{EE}^{1-} from calculations B (Bare, corresponding to the usual K-matrix approach) and D (Dressed, the full Dressed K-matrix results) are rather similar in the vicinity of threshold.

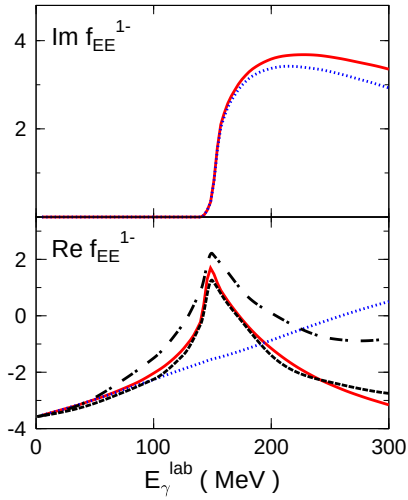

Fig. 6. The f_{EE}^{1-} partial amplitude of Compton scattering on the proton in units $10^{-4}/m_\pi$. Solid line: dressed K-matrix, D; dotted line: bare K-matrix, B. Also shown are the results of the dispersion analyses of Ref. [12] (dash-dots) and Ref. [13] (dashed).

The polarizabilities characterize the response of the nucleon to an externally applied electromagnetic field [14, 15]. They can be defined as coefficients in a low-energy expansion of the cross section or partial amplitudes of Compton scattering. Since gauge invariance, unitarity, crossing and CPT symmetries are fulfilled in both models the Thompson limit at vanishing photon energy is reproduced. Our results for the electric, magnetic and spin polarizabilities of the proton are given in Table I, where they are compared with the results given in Refs. [14, 16] and with the values extracted from recent experiments. The contribution from the t-channel π^0-exchange diagram has been subtracted. The effect of the dressing on the polarizabilities can be seen by comparing the values given in columns D (dressed) and B (bare). In particular, the dressing tends to decrease α while increasing β. Among the spin polarizabilities, γ_{E1} is affected much more than the other γ's. The effect of the additional "cusp" $\gamma\gamma NN$ contact term [7], strongly influences the electric polarizabilities rather than the magnetic ones. This is because the "cusp" contact term affects primarily the electric partial amplitude f^{1-}_{EE} (corresponding to the total angular momentum and parity of the intermediate state $J^\pi = 1/2^-$) rather than the magnetic amplitude f^{1-}_{MM} ($J^\pi = 1/2^+$).

TABLE I

Polarizabilities of the proton. The units are 10^{-4}fm^3 for α and β and 10^{-4}fm^4 for the γ's (the anomalous π^0 contribution is subtracted). The first two columns contain the polarizabilities obtained from the present calculation; D (full, dressed) and B (bare K-matrix). The two columns named χPT contain the polarizabilities calculated in the chiral perturbation theory [14, 16]. Results of recent dispersion analyses are given in the last column (Ref. [17] for α and β and Ref. [18] for the γ's).

			χPT		DA
	D	B	Gel00	Hem98	
α	12.1	15.5	10.5	16.4	11.9
β	2.4	1.7	3.5	9.1	1.9
γ_{E1}	−5.0	−1.7	−1.9	−5.4	−4.3
γ_{M1}	3.4	3.8	0.4	1.4	2.9
γ_{E2}	1.1	1.0	1.9	1.0	2.2
γ_{M2}	−1.8	−2.3	0.7	1.0	0.0
γ_0	2.4	−0.9	−1.1	2.0	−0.8
γ_π	11.4	8.9	3.5	6.8	9.4

Of special interest is to check whether polarizabilities as extracted form the low energy behavior of the amplitude are in agreement with the values as extracted from energy weighted sum-rules. The derivation of sum-rules

is based on the fact that the amplitudes obey certain symmetries where analyticity is of particular importance. This comparison is still in progress and results will be published in a forthcoming paper [10]. Preliminary results indicate that the different sum rules are obeyed, with the exception of the sum rule for the spin polarizability γ_0. This may be due to an incomplete dressing of the Δ-resonance in the present calculational scheme.

5. Medium modifications of the Δ resonance

The properties of the Δ in the nuclear medium are calculated [19] in a relativistic framework for symmetrical (*i.e.* $T = 0$) homogenous nuclear matter, along the lines of Refs. [20–22]. The medium modifications are expressed through the dressing of the Δ propagator. The effects of the medium are investigated using different levels of approximation. The imaginary part of the Δ self-energy (or the Δ decay width) is calculated in different models for the nuclear medium. Dispersion relations are used to determine the real part (mass modification) of the Δ self-energy in a manner similar to the dressed K-matrix approach, however without requiring self consistency.

In dressing the in-medium Δ-resonance we concentrate on the dominant spin-3/2 component of the propagator. The spin-3/2 component of the self-energy has the structure

$$\Sigma_\Delta^{3/2} = C_\Delta(p_\Delta) + D_\Delta(p_\Delta)\, \not{p}_\Delta \,, \tag{4}$$

where $p_\Delta = (p_\Delta^0, \vec{p}_\Delta)$. Note that in vacuum $C_\Delta(p_\Delta)$ and $D_\Delta(p_\Delta)$ are functions of the invariant $W_\Delta = (p_\Delta^2)^{1/2}$ only, while in the medium these functions acquire additional dependences on the 3-momentum $|\vec{p}_\Delta|$ and the nuclear density ρ.

The width of the resonance is defined by the imaginary part of the self-energy at the pole position ($W_\Delta = M_\Delta$). The contribution to the self-energy for a Δ decaying into a nucleon and a pion is

$$-i\,(\Sigma_\Delta)_{\mu\nu} = \Big(\frac{f_{\pi N\Delta}}{m_\pi}\Big)^2 \sum_{a=1,2,3} \int \frac{d^4k}{(2\pi)^4} q_\mu T_a^\dagger G_N(k)(-q_\nu) T_a D_\pi(q), \tag{5}$$

where $q = p_\Delta - k$, and $G_N(k)$ and $D_\pi(q)$ are the nucleon and pion propagators, the structure of which depends on the model used for the nuclear medium.

In the following two sections the density dependence of two contributions to the width of the Δ-resonance, the decay and spreading width, are discussed in a Fermi gas model. In a subsequent section the effect of the mean field is included within the $\sigma\omega$-model of Walecka [23].

5.1. Decay width of the Δ-resonance

In a simple Fermi gas model Δ decay, corrected for the Pauli principle, can be written as

$$\Gamma_\Delta^D(p_\Delta) = \frac{f_{\pi N\Delta}^2\,(E_{k_\pi} + M_N)\,k_\pi^2}{24\pi m_\pi^2\,|\vec{p}_\Delta|}\,[E_+ - \max(E_-, E_{\rm F})]\;\theta(E_+ - E_{\rm F})\,, \quad (6)$$

where $E_\pm = (p_\Delta^0 E_{k_\pi} \pm |\vec{p}_\Delta| k_\pi)/W_\Delta$ and k_π is the pion (nucleon) on-shell 3-momentum in the loop. The width becomes $|\vec{p}_\Delta|$- and density-dependent. In the limit $|\vec{p}_\Delta| \to 0$ the width reduces to its vacuum value if $E_{k_\pi} > E_{\rm F}$, and to zero if $E_{k_\pi} \le E_{\rm F}$;

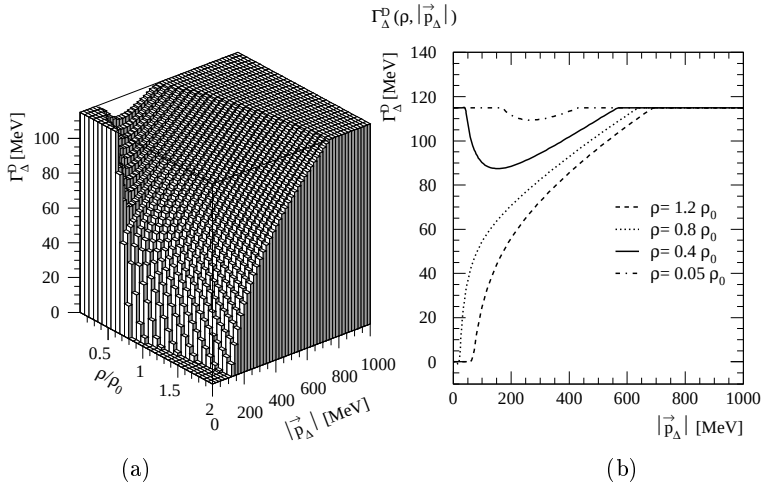

(a) (b)

Fig. 7. (a) In the left panel the Δ decay width is depicted as a function of the density ρ (in units of the equilibrium density ρ_0 [$k_{\rm F}^0 = 1.333$ fm^{-1}]) and the Δ 3-momentum $|\vec{p}_\Delta|$ at $W_\Delta = 1232$ MeV calculated in the Fermi-gas model. (b) The right panel shows the results for this calculation as a function of the Δ 3-momentum $|\vec{p}_\Delta|$ for the 4 different densities.

In Fig. 7(a) the full dependence on ρ and $|\vec{p}_\Delta|$ is shown for $W_\Delta = 1232$ MeV. The results at densities 1.2, 0.8, 0.4 and 0.05 times normal nuclear matter density ρ_0 ($k_{\rm F}^0 = 1.333$ fm^{-1}) are plotted separately in Fig. 7(b). At high Δ-momenta and low densities the energy of the decay nucleon lies well above the Fermi energy, and no blocking occurs. At somewhat lower momenta of the Δ part of the momenta of the decay nucleon are Pauli blocked. With increasing density this blocking may become complete for the lowest Δ-momenta making the Δ unable to decay into a pion–nucleon pair (see dashed and dotted curves in Fig. 7(b)). These phase–space considerations result in a strong energy-dependence of the Δ decay width.

5.2. Spreading width

In the nuclear medium the pion will strongly interact with the surrounding baryons creating nucleon–hole and Δ–hole excitations. This can be taken into account by dressing the pion propagator with the proper pion self-energy

$$D_\pi(q) = \frac{1}{q^2 - m_\pi^2 - \Pi_\pi(q) + i\varepsilon} \ , \tag{7}$$

where $\Pi_\pi(q) = \Pi_{\rm ph}(q) + \Pi_{\Delta h}(q)$ is the polarization self-energy of the pion. In our calculations we limit ourselves to forward and backward scattered particle–hole excitations, and omit anti-nucleon excitations and Δ–hole states. In principle, a complete calculation of the Δ–hole states would require self-consistency between the pion and Δ self-energies, which falls outside the scope of this work. We use the pion–nucleon pseudo-vector coupling with the πNN-coupling constant $f_{\pi NN} = 1.01$ [21].

When summing the series of particle–hole bubbles in the pion-self energy, the effects of short-range correlations are important. These short-range correlations are accounted for in the standard way by introducing the Landau–Migdal parameter $g'_{NN} = 0.6$ [24].

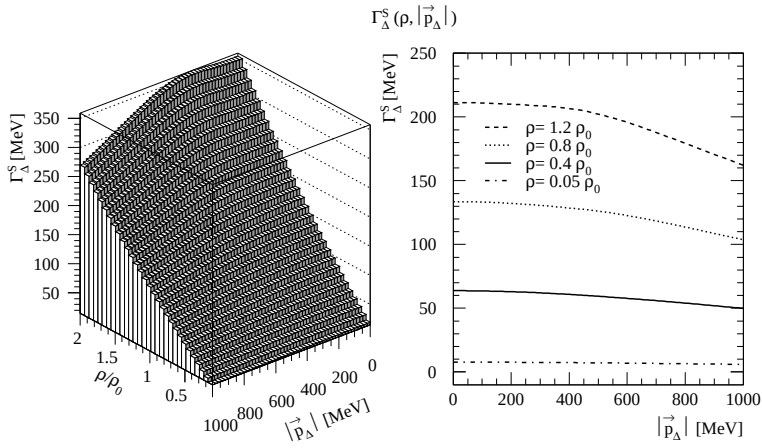

(a) (b)

Fig. 8. (a) In the left panel the spreading width is depicted as a function of the density ρ (in units of the equilibrium density ρ_0 [$k_{\rm F}^0 = 1.333\,{\rm fm}^{-1}$]) and the Δ 3-momentum $|\vec{p}_\Delta|$ at $W_\Delta = 1232$ MeV calculated in the Fermi-gas model. (b) The right panel shows the results for this calculation as a function of the Δ 3-momentum $|\vec{p}_\Delta|$ for the 4 different densities.

Using the pion propagator from Eq. (7) with the pion self-energy $\Pi_{\rm ph}$ in Eq. (5) the spreading width of the Δ-resonance in the medium can be calculated. The results are shown in Fig. 8. The spreading width is roughly

proportional to the density, which can be understood on the basis of the phase space available for the hole states. As can be seen from Fig. 8(b) it is only weakly dependent on the 3-momentum $|\vec{p}_\Delta|$. Also the dependence on W_Δ turns out to be weak. The total width of the Δ in this non-interacting Fermi-sea of nucleons is given by the sum of this spreading width and the Pauli-corrected decay width from the previous section.

5.3. Mean-field effects in the nucleon and Δ self-energy

A refinement to the free Fermi-gas model can be made using the Walecka $\sigma\omega$-model [23] in the mean-field approximation. Here the σ- and ω-meson couple to the nucleon resulting in the (classical) mean scalar and vector fields $\langle \Phi_s \rangle$ and $\langle V^\mu \rangle$.

In order to assess the sensitivity of the results to the mean-field parameters we have performed calculations taking 2 parameter sets from [25], henceforth called set I and II. Set I, called QHD-I in [25], results from a pure mean-field approximation to the binding energy. The ratios of coupling constants and meson masses have values $C_s^2 = (g_s^N M_N/m_s)^2 = 267.1$, $C_v^2 = (g_v^N M_N/m_v)^2 = 195.9$. The nuclear matter equilibrium density is at $k_{\rm F}^0 = 1.42$ fm^{-1}, with binding energy 15.75 MeV and an effective nucleon mass $M_N^*/M_N = 0.56$ at ρ_0. Set II, called the relativistic Hartree approximation in [25], takes into account vacuum fluctuation corrections to the binding energy. The parameters are $C_s^2 = 228.2$, $C_v^2 = 147.8$. The equilibrium density is taken at $k_{\rm F}^0 = 1.30$ fm^{-1}, with a binding energy of 15.75 MeV leading to an effective nucleon mass $M_N^*/M_N = 0.73$ at equilibrium density. The full density dependence of the effective nucleon masses in both cases are shown in Fig. 9. In both cases we see a strong reduction of the effective nucleon mass with increasing density. In the extended mean-field model of Ref. [20] the Δ is assumed to move in the mean σ and ω fields. The mean-field contributions to the Δ self-energy can be treated in an analogous way as for the nucleon, *i.e.* they are absorbed in the effective Δ mass $M_\Delta^\star$ and 4-momentum $p_\Delta^\star$. Here we employ the so-called universal couplings [20], and as a result the Δ effective mass $M_\Delta^\star(\rho)$ may be expressed as $M_\Delta^\star(\rho) = M_\Delta - (M_N - M_N^\star)$.

The effect of these mean-field modifications for the decay width Γ_Δ^D and the spreading width Γ_Δ^S at the on-shell point $W_\Delta^\star = M_\Delta^\star(\rho)$ for both parameter sets are depicted in Fig. 10. It is seen that the structure of the decay width hardly changes when effective masses are introduced; only the limiting value at large $|\vec{p}_\Delta|$ now becomes density-dependent. Because of the stronger reduction of the effective masses the Pauli-blocking is more pronounced using parameter set I. The mean-field effects result in an overall reduction of the spreading width as compared to the Fermi-gas calculation

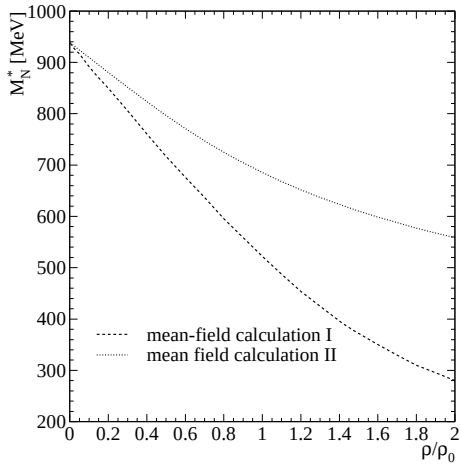

Fig. 9. The effective nucleon mass M_N^* as a function of the density ρ (in units of the equilibrium density ρ_0 (value depending on the model)) for the mean-field calculations I and II as explained in Section 5.3.

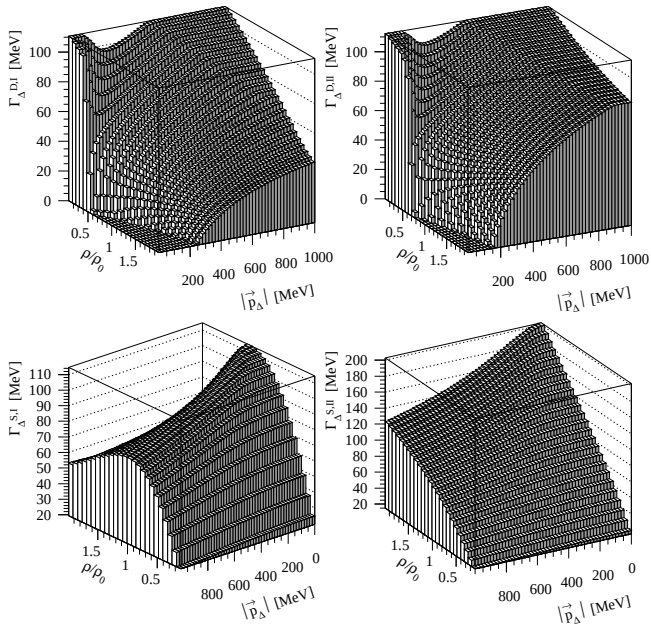

Fig. 10. The Pauli-corrected Δ decay width Γ_Δ^D and the spreading width Γ_Δ^S in function of the density ρ (in units of the equilibrium density ρ_0 (value depending on the model)) and the Δ 3-momentum $|\vec{p}_\Delta|$ calculated in the mean-field model I and II (marked by index I and II, respectively) at $W_\Delta^\star = M_\Delta^\star(\rho)$.

(see Fig. 8). For the relevant nuclear densities $\rho/\rho_0 \leq 1.2$, this reduction is stronger at larger densities. For larger densities the spreading width saturates and eventually decreases in both mean-field models. The mean-field model I yields a maximal spreading width at around the equilibrium density. In the mean-field model II, the spreading width saturates at much larger densities.

5.4. Real part of the Δ self-energy

The full width, *i.e.* the sum of the decay and spreading widths, corresponds to the imaginary part of the Δ self-energy. This imaginary part generates a contribution to the real part of the Δ self-energy, which can in general be obtained via a dispersion relation. We make the assumption that an unsubtracted dispersion relation holds at fixed values of $|\vec{p}_\Delta|$. The propagator is renormalized in such a way that in vacuum it has a pole at the physical mass $M_\Delta = 1.232$ GeV with unit residue.

6. Coherent Compton scattering

Coherent Compton scattering on nuclei in the region of the Δ resonance is of considerable interest. The reaction allows one to study the propagation and decay of the Δ in the nuclear medium. In particular the shift of the pole position and a change of the width of the Δ peak, reflect sensitively in the cross section and polarization observables. For a comprehensive review on Compton scattering we refer to the recent reference [26].

The amplitude for the process of Compton scattering on a finite nucleus is calculated in the impulse approximation. We apply the so-called factorization approximation (see [27], ch.11, sect.2) which was shown to work well in pion photoproduction [28–30] and pion scattering [31, 32] on nuclei, in particular for light nuclei where the nuclear wave function is well described by an harmonic oscillator model. A large part of the effects of the Fermi-motion are accounted for by evaluating the amplitude on a nucleon moving with the effective momentum p ($p' = p + q$) in the initial (final) state, where $q = k - k'$ is the momentum transfer. The momentum p is taken in such a way that the energy–momentum conservation for the γN scattering holds. The amplitude in this approximation is written as

$$K_A = A \, \langle \, T_N(\vec{p}) \, \rangle \, F_\rho(q) \, , \tag{8}$$

where $F_\rho(q)$ is the Fourier-transform of the density distribution (form factor). In Eq. (8), the form factor of the $1s$- $1p$-shell nuclei with $Z = N = A/2$ is constructed on the basis of the experimental charge densities in [33] (see Table V therein), correcting for proton finite size effects and assuming equal proton and neutron densities. $\langle T_N \rangle$ is the spin averaged single-nucleon amplitude.

The single-nucleon amplitude is decomposed into one part which corresponds to the amplitude on the free nucleon, plus a term which accounts for the modification of the Δ-resonance in the medium, *i.e.*

$$T_N = T_N^{\text{free}} + \left(K_N^{\Delta_d} - K_N^{\Delta_f} \right). \tag{9}$$

The first term is the T-matrix for Compton scattering on the free nucleon; the term between brackets accounts for the nuclear-medium modification of the Δ-resonance. To avoid double counting the vacuum contribution is subtracted.

The T-matrix for Compton scattering off a free proton, T_N^{free}, is calculated in a K-matrix model as described in Section 2. The main difference of the present calculation from that of Ref. [4] is that the Δ is treated as a genuine spin-3/2 resonance [5] in order to be compatible with the present treatment of the in-medium Δ-resonance. The change in the structure of the $\gamma N\Delta$ and $\pi N\Delta$-vertices necessitated modification of parameters of the ρ and σ exchanges in the t-channel. A comparable fit to the data as in Ref. [4] could be obtained. In the dressed Δ-contribution $K_N^{\Delta_d}$ only the s-type tree-level contribution is taken into account, using the medium-modified Δ propagator as defined previously.

Cross sections have been calculated for ^{4}He and ^{12}C at several densities to investigate medium effects. To compare with data an average over density (ρ_A), based on the Local Density Approximation (LDA), has been performed. The density profile (ρ_A) was taken consistently with the form factor.

In Fig. 11 we have plotted, for various nuclear densities, the cross section and photon asymmetry for Compton scattering on ^{4}He in mean-field model I, both at fixed $\theta_{\text{lab}} = 37^\circ$ and $E_{\gamma\text{lab}} = 206$ MeV. The results show a strong density dependence. In order to obtain more insight we have plotted in the upper panels of Fig. 12 the values of the 3-momentum $|\vec{p}_\Delta|$ and (kinematical) invariant mass W_Δ of the Δ as enter in the calculations presented in Fig. 11. In the lower panels we show the real and imaginary part of the Δ self-energy.

One may want to compare the results we have obtained for the in-medium correction to the self-energy of the Δ-resonance to results obtained in Ref. [30] from fitting to coherent pion photoproduction. In making this comparison one has to be careful since we include explicitly in calculations the density and momentum dependencies of the Δ self-energy, while both effects are neglected in [30]. Keeping this in mind, the results of [30] agree reasonably well with ours.

In Fig. 12 at $E_\gamma = 350$ MeV the real part of the self-energy is of the order of 45 MeV (taking the $\rho = 0.8\rho_0$ result at 40°), while Ref. [30] finds a

value of 30 MeV. Both figures show that this value decreases towards lower energies to vanish in our case at about 200 MeV photons, while in Ref. [30] there is an additional bump at the lower energies.

The imaginary part shows a similar agreement. Plotted in Ref. [30] is the modification of the free width which is about −60 MeV and is taken energy independent. At a photon energy of 350 MeV the additional in-medium contribution is about −55 MeV giving −115 MeV for the imaginary part of the self-energy, to decrease (in absolute magnitude) for lower energies. The values we obtain are similar (see Fig. 12), however with a slower decrease towards lower energies. Besides, at these lower energies we find that the density dependence becomes quite significant and should not be ignored.

Much of the density dependence of the cross sections in Fig. 11 can be understood from the density dependence of the imaginary part of the Δ self-energy. At a photon energy of 206 MeV one is relatively far from the peak of

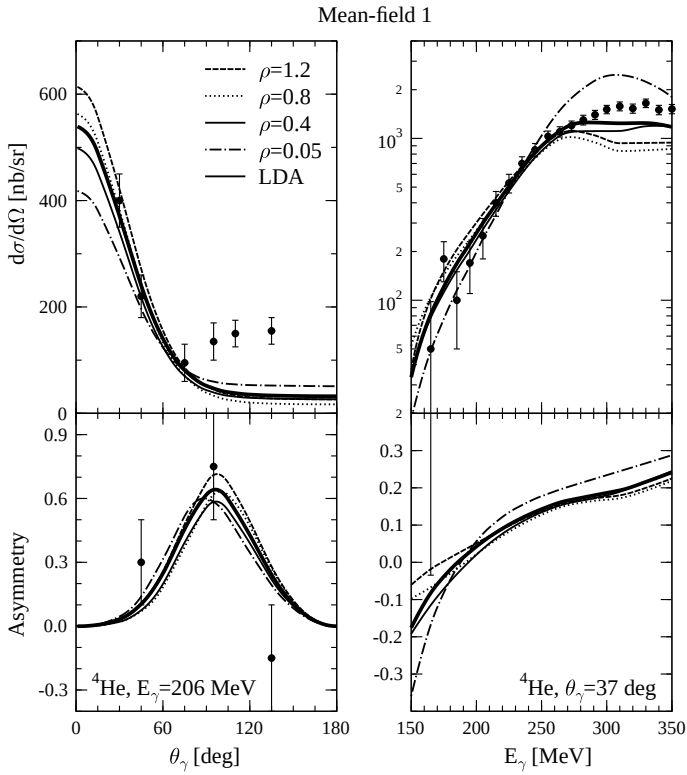

Fig. 11. Differential cross section and photon asymmetry for Compton scattering off ^{4}He at an energy of 206 MeV as a function of angle and at an angle of 37° as a function of energy. Densities are given in units of saturation density. Data are taken from [35].

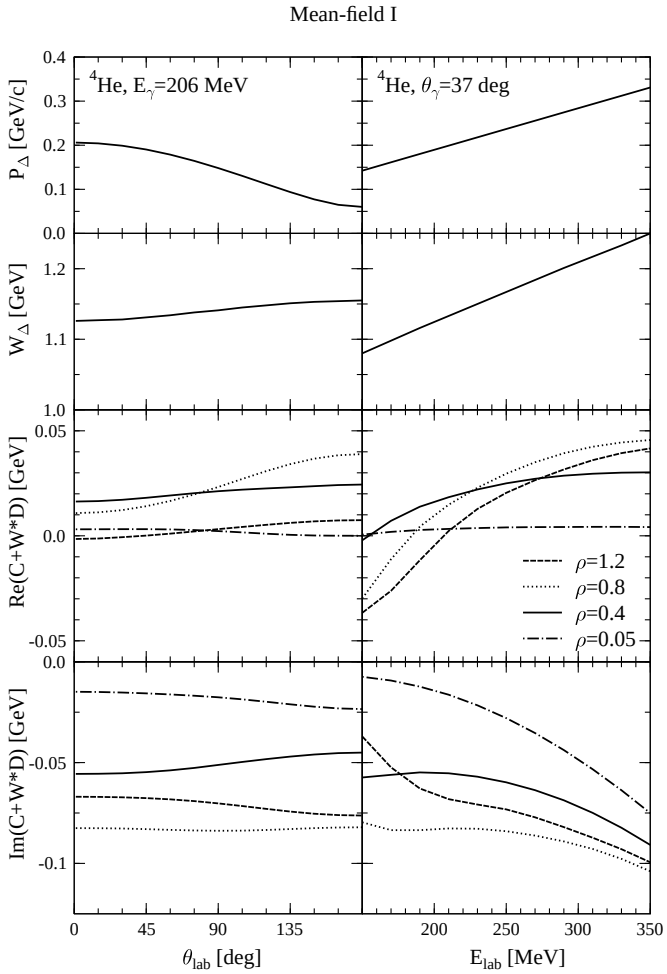

Fig. 12. Values of the parameters which define the self-energy of the Δ-resonance evaluated at the Δ invariant mass (W_Δ) and three momentum ($|\vec{p}_\Delta|$) appropriate for Compton scattering off ^{4}He as shown in Fig. 11.

the Δ-resonance. An increase in the width of the resonance therefore results in an increase of the cross section at this energy. The opposite happens when one approaches the peak of the resonance, where the cross section decreases with density. The data show clear evidence that this is indeed the correct mechanism, at 206 MeV the vacuum calculation falls below the data while the LDA result shows a good correspondence with the data at forward angles. Near the resonance the vacuum calculation overestimates the data by a factor 2 while the LDA result gives a much better prediction or even lies below. The sharp fall-off of the cross section with angle is mostly due to the form factor which falls off strongly with increasing momentum transfer.

At backward angles the cross section is not reproduced, which is probably due to the double-scattering contribution which is missing from the present calculations. The photon asymmetry at 206 MeV shows only a minor density dependence as compared to the error bars on the data.

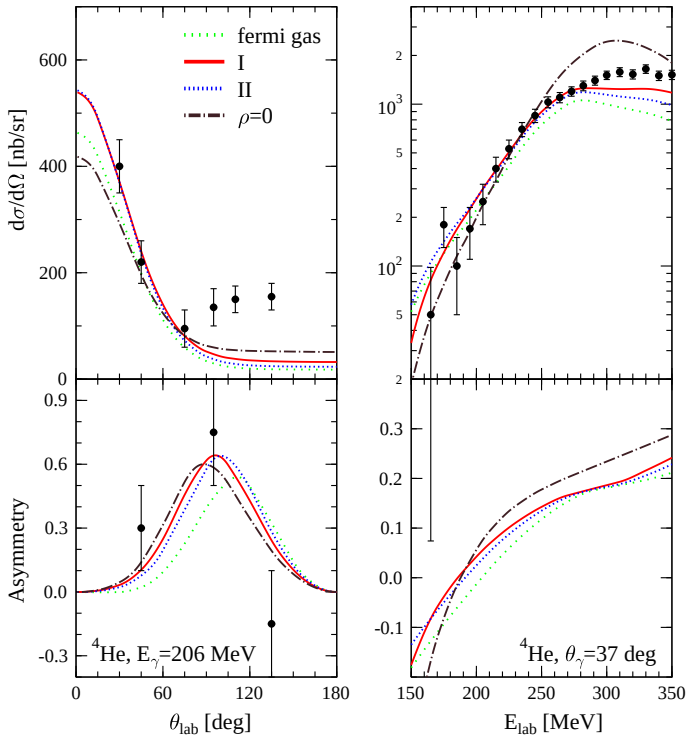

Fig. 13. LDA calculation of coherent Compton scattering off ^{4}He in the Fermi-gas model and the mean-field models I and II. The data are from Ref. [34].

In Fig. 13 we compare the ^{4}He cross section and asymmetry with LDA calculations for the Fermi-gas and mean-field calculations I and II. The Fermi-gas calculation undershoots the data at small angles for $E_\gamma = 206$ MeV and at large energies for $\theta_\gamma = 37^\circ$, and deviates from the asymmetry data points. The mean-field calculations tend to improve this.

The cross sections for ^{12}C is shown in Fig. 14. Because of the larger radius of ^{12}C the cross section falls off faster with angle than that for ^{4}He. The drop in the cross section at energies beyond 250 MeV is partly due to an increased width of the Δ-resonance and partly due to the form factor cutting the cross section at larger momentum transfers. This effect is also seen in the data.

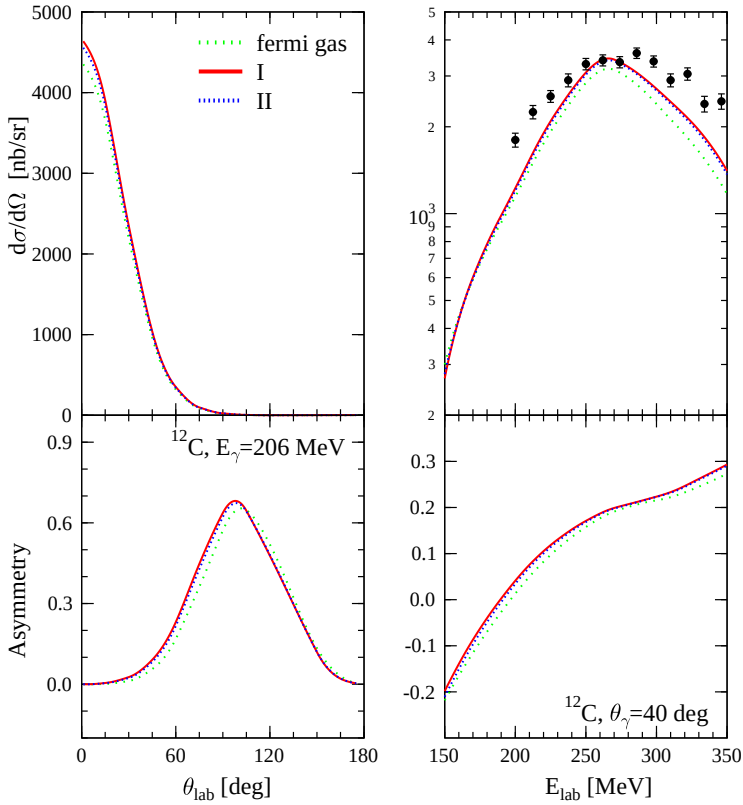

Fig. 14. Same as Fig. 13 but for ^{12}C. The data are from Ref. [34].

7. Summary and conclusions

Results are presented for Compton scattering on a free proton as well as on a nucleus. For processes on the proton the usual K-matrix model as well as the recently developed dressed K-matrix model are discussed. In the latter approach the real self energies and vertex functions are obtained from the imaginary parts using dispersion relations imposing self-consistency conditions. It is indicated that such an approach is essential to understand features seen in the data, in particular at energies around and below the pion production threshold.

It is shown that 200–300 MeV coherent Compton scattering is sensitive to the in-medium modification of the properties of the Δ-resonance. The imaginary part of the Δ self-energy in the nuclear medium includes two contributions, the decay width and the spreading width, which show opposite dependences on the density. The net effect for realistic nuclei of these counteracting mechanisms is an increase of the width. The real part, calculated

using dispersion integrals, is small. These predictions for the modification of the Δ in the nuclear medium are shown to give good predictions for the differential Compton cross section at forward angles for ^{4}He and ^{12}C. The present one-body reaction mechanism is unable to describe the data at backward angles. In order to improve this, it is imperative that multiple scattering should be incorporated in the model.

O.S. thanks the Stichting voor Fundamenteel Onderzoek der Materie (FOM) for their financial support. A.Yu. K. thanks the Foundation for Fundamental Research of the Netherlands (NWO) for financial support. The work of L. V.D. and D. V.N. was supported by the Fund for Scientific Research — Flanders (FWO) and the Research Board of Ghent University. S.K. thanks the National Sciences and Engineering Research Council of Canada for their financial support.

REFERENCES

[1] P.F. A. Goudsmit, H.J. Leisi, E. Matsinos, B.L. Birbrair, A.B. Gridnev, *Nucl. Phys.* **A575**, 673 (1994).
[2] O. Scholten, A.Yu. Korchin, V. Pascalutsa, D. Van Neck, *Phys. Lett.* **B384**, 13 (1996).
[3] T. Feuster, U. Mosel, *Phys. Rev.* **C58**, 457 (1998); *Phys. Rev.* **C59**, 460 (1999).
[4] A.Yu. Korchin, O. Scholten, R.G.E. Timmermans, *Phys. Lett.* **B438**, 1 (1998).
[5] V. Pascalutsa, *Phys. Lett.* **B503**, 85 (2001).
[6] S. Kondratyuk, O. Scholten, *Phys. Rev.* **C59**, 1070 (1999); *Phys. Rev.* **C62**, 025203 (2000).
[7] S. Kondratyuk, O. Scholten, *Nucl. Phys.* **A677**, 396 (2000).
[8] S. Kondratyuk, O. Scholten, *Nucl. Phys.* **A680**, 175c (2001).
[9] S. Kondratyuk, O. Scholten, *Phys. Rev.* **C64**, 024005 (2001).
[10] S. Kondratyuk, O. Scholten, `nucl-th/0109038`.
[11] E.L. Hallin *et al.*, *Phys. Rev.* **C48**, 1497 (1993).
[12] W. Pfeil, H. Rollnik, S. Stankowski, *Nucl. Phys.* **B73**, 166 (1974).
[13] J.C. Bergstrom, E.L. Hallin, *Phys. Rev.* **C48**, 1508 (1993).
[14] T.R. Hemmert, B.R. Holstein, J. Kambor, *Phys. Rev.* **D57**, 5746 (1998).
[15] B.R. Holstein, `hep-ph/0010129`.
[16] G.C. Gellas, T.R. Hemmert, Ulf-G. Meissner, *Phys. Rev. Lett.* **85**, 14 (2000).
[17] A.I. L'vov, V.A. Petrun'kin, M. Schumacher, *Phys. Rev.* **C55**, 359 (1997).
[18] D. Drechsel, M. Gorchtein, B. Pasquini, M. Vanderhaeghen, *Phys. Rev.* **C61**, 015204 (2000).
[19] L. Van Daele *et al.*, *Phys. Rev.* **C65**, 014613 (2001).
[20] T. Herbert, K. Wehrberger, F. Beck, *Nucl. Phys.* **A541**, 699 (1992).
[21] H. Kim, S. Schramm, S.H. Lee, *Phys. Rev.* **C56**, 1582 (1997).

[22] L. Liu, X. Luo, Q. Zhou, W. Chen, M. Nakano, *Phys. Rev.* **C51**, 3421 (1995).
[23] J.D. Walecka, *Ann. Phys.* **83**, 491 (1974).
[24] T. Suzuki, H. Sakai, *Phys. Lett.* **B455**, 25 (1999).
[25] B.D. Serot, J.D Walecka, *Adv. Nucl. Phys.* **16**, 1 (1986).
[26] M.-Th. Hütt, A.I. L'vov, A.I. Milstein, M. Schumacher, *Phys. Rep.* **323**, 457 (2000).
[27] M.L. Goldberger, K.M. Watson, *Collision Theory*, John Wiley and Sons, Inc., 1964.
[28] L. Tiator, A.K. Rej, D. Drechsel, *Nucl. Phys.* **A333**, 343 (1980).
[29] R.A. Eramzhyan, M. Gmitro, S.S. Kamalov, *Phys. Rev.* **C41**, 2685 (1990).
[30] D. Drechsel, L. Tiator, S.S. Kamalov, Shin Nan Yang *Nucl. Phys.* **A660**, 423 (1999).
[31] R.H. Landau, S.C. Phatak, F. Tabakin, *Ann. Phys.* **78**, 299 (1973).
[32] R.H. Landau, A. W. Thomas, *Phys. Lett.* **B61**, 361 (1976).
[33] H. De Vries, C.W. De Jager, C. De Vries, *At. Data Nucl. Data Tables* **36**, 495 (1987).
[34] F. Wissmann *et al. Phys. Lett.* **B335**, 119 (1994).
[35] A. Kraus, O. Selke, F. Wissmann *et al.*, *Phys. Lett.* **B432**, 45 (1998).